JOURNAL OF GEOPHYSICAL RESEARCH, VOL. 92, NO. A4, PAGES 3273–3283, APRIL 1, 1987

The Equatorward Boundary of Auroral Ion Precipitation

M. S. GUSSENHOVEN AND D. A. HARDY

Air Force Geophysics Laboratory, Hanscom Air Force Base, Massachusetts

N. HEINEMANN

Physics Department, Boston College, Chestnut Hill, Massachusetts

The data from the SSJ/4 detector on the Defense Meteorological Satellite Program (DMSP) F6 satellite are used to study the difference in the location of the equatorward boundaries of auroral ion and electron precipitation, and the variation in the difference with magnetic local time and activity. Large geometric factors of the ion sensors of the SSJ/4 detector make identification of the ion boundary unambiguous in most cases. In this study, approximately 900 boundaries each for electrons and ions were determined from all DMSP F6 auroral passes in January of 1983. The boundaries occur over local times from 0400 to 0700 on the morningside of the oval and from 1700 to 2100 on the eveningside. The ion and electron boundaries both move systematically to lower latitudes with increasing magnetic activity, as measured by *Kp*. Over the evening sector sampled, the ion boundary is on average 1.4° equatorward of the electron boundary, with the difference commonly ranging up to 3°. For the morning sector sampled, the ion boundary is on average 2.6° poleward of the electron boundary with a significant number of cases with differences above 5.0°. The separation between the electron and ion boundaries is not dependent on *Kp* but does increase with MLT from midnight toward noon on both the morningside and the eveningside of the oval. The separation in boundaries can be explained by motion in a large-scale, quasi-static convection electric field if the time for development of the ion boundary is explicitly taken into account and if ion pitch angle diffusion is highly energy dependent.

1. INTRODUCTION

A number of statistical studies have been published on the location of the equatorward boundary of auroral electron precipitation measured at low altitude, and the systematic variation of the boundary with geomagnetic activity, substorm, and solar wind parameters (see *Kamide and Winningham* [1977], *Gussenhoven et al.* [1981, 1983], *Hardy et al.* [1981], *Makita et al.* [1983], *Sauvaud et al.* [1983], and *Nakai et al.* [1986]; see also the recent review article by *Feldstein and Galperin* [1985] and references therein). In several of these studies the systematic boundary variations were used to evaluate models of the large-scale, quasi-stationary, magnetospheric electric field by associating the low-altitude precipitating electron boundaries with Alfvén layers at high altitudes (and specifically the inner edge of the central plasma sheet). For this the following assumptions are made: (1) The electric field is slowly varying. (2) The polarization electric field associated with any difference in the auroral ion and electron motions is small, or is neutralized by another particle population, or is included in the model field (i.e., the model field is self-consistent, by accident or otherwise). (3) The electron pitch angle diffusion is slow enough not to exhaust the density in a flux tube in the time required for formation of a convection boundary but is fast enough to maintain a sufficient flux level in the loss cone so that the bulk motions of the electrons can be followed with the loss cone population. On a statistical basis these assumptions have proved to be reasonably good for electrons. *Fontaine and Blanc* [1983] showed that electron boundaries established under the combination of convection and strong pitch angle diffusion are dominated by depletion of the flux tube and are not in agreement with measured values (they are too high at low altitudes). The first statistical maps of the measured electric field at geosynchronous altitude [*Baumjohann et al.*, 1985] are in reasonable agreement with models that give good predictions for the low-altitude electron precipitation boundaries due to convection only.

Despite the success of relating the low-altitude electron boundaries to magnetospheric processes, similar analysis efforts have not been made using low-altitude ion boundaries. Auroral ion fluxes are smaller than electron fluxes by 1–2 orders of magnitude in the auroral energy range (100 eV to 50 keV), but ion detectors on polar-orbiting satellites typically have had the same geometric factors as electron detectors. As a result the ions have been measured at low count rates that, in turn, have made the determination of the ion boundaries difficult.

The most systematic determinations of the extent of ion precipitation and the relationship of electron and proton fluxes have been made photometrically, and principally from the ground (see the review by *Eather* [1967]; also *Vallance-Jones* [1974, 1982], *Fukunishi* [1975], and *Lambert and Sutcliffe* [1981]). These authors show that proton diffuse aurora, as measured by H_α and H_β emissions, can extend below the electron diffuse aurora on the eveningside of the oval and that the electron diffuse aurora dominates on the morningside.

Precipitating particle measurements at low altitudes have given less clear results (see the review by *Hultqvist* [1979] and references therein). *Lui et al.* [1977] found the thermal plasma and ion equatorward boundaries to be in good agreement with one another on the eveningside of the oval. This conclusion was qualified since their detectors extended in energy only up to 26 keV and the energy flux was still increasing at

Paper number 6A8735.
0148-0227/87/006A-8735$05.00

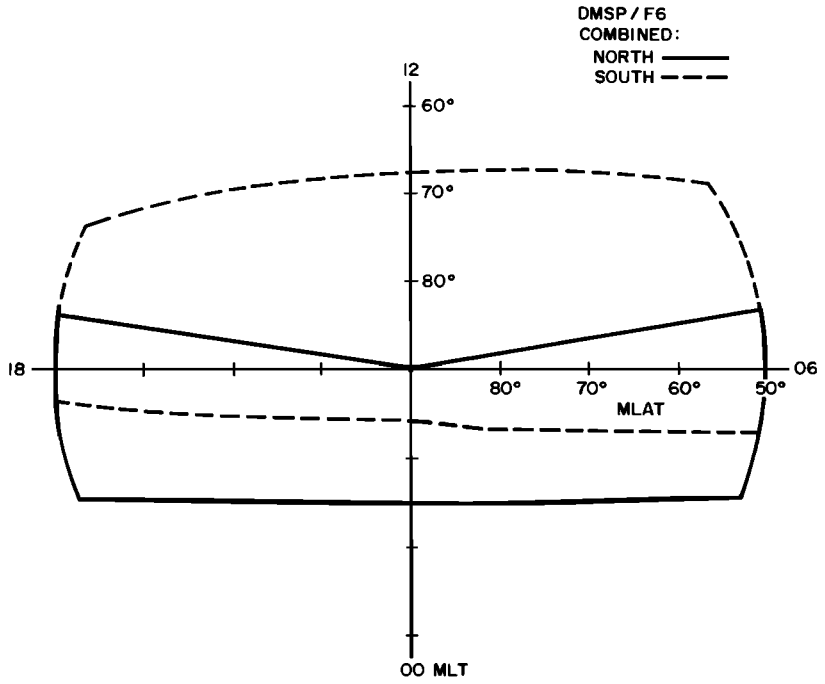

Fig. 1. Orbital coverage in magnetic local time and corrected geomagnetic latitude for DMSP F6. The solid (dashed) line encloses the regions covered in the north (south) pole.

the boundary. *Hultqvist* [1979] compared evening ion boundaries to published measurements of the postmidnight plasmapause and found the ion boundaries generally higher. *Sauvaud et al.* [1981] studied ion precipitation on the morningside of the oval. There they found a very low energy population on the equatorward edge of the precipitation and concluded that it originates in the ionosphere, not the central plasma sheet. Other evidence for this has been given by *Galperin et al.* [1978] and *Sauvaud et al.* [1985]. If the same assumptions used to explain electron boundaries hold for proton transport, the particle motion resulting from the convection electric field will bring the proton population closer to the earth at all local times [*Cowley and Ashour-Abdalla*, 1976*a*, *b*; *Ejiri*, 1978; *Southwood and Kaye*, 1979]. Low-altitude equatorward proton boundaries would then be found below the corresponding electron boundaries at all magnetic local times.

At high altitudes, *Smith and Hoffman* [1974] have demonstrated the existence of "proton noses" in the dusk sector. The noses consist of kilovolt protons found within the plasmapause and at smaller radial distances than the plasma sheet electrons. The fact that protons are not as far inside the plasmasphere as their motion in a constant dawn-to-dusk electric field permits led *Ejiri et al.* [1978] to suggest modifications in the electric field model. The pitch angle distributions of the nose protons are strongly peaked at 90°. Thus the flux in the loss cone would be small and probably would produce no measurable signature at low altitudes.

Statistical maps of the moments of the electron and ion distributions measured by the SCATHA satellite at near-geosynchronous altitudes (5.5 to 8.5 R_E) by *Mullen and Gussenhoven* [1983] show a well-defined density peak for electrons in the 100-eV to 20-keV energy range, at 5–6 R_E, and between local times from 1900 to 0300 hours (through midnight). There is no corresponding drop-off in the ion density at altitudes below the peak in the electron density. This indicates that the plasma sheet ions, at least for these local times, access regions nearer the earth than electrons.

Many of the studies listed above have attempted to establish a consistent picture of transport and loss in the inner magnetosphere that applies separately to ions and electrons. In addition, there are magnetospheric processes that are directly associated with the difference between the location of the inner edge of the electron and ion plasma sheet populations. The difference in ion and electron trajectories generates polarization currents that alter the imposed electric field. Polarization electric fields created in this fashion have been suggested as the source for the region 2 Birkeland currents (see *Alfvén and Falthammar* [1963] and *Schield et al.* [1969]; see also the review article by *Stern* [1983]). *Ashour-Abdalla and Thorne* [1978], on the basis of the observations of the near-coincidence of the regions of ion and electron diffuse aurora, suggested that the energy source for the strong pitch angle diffusion of ions in the plasma sheet reservoir is broadband electrostatic noise generated by field-aligned currents.

In this study we use the Defense Meteorological Satellite Program (DMSP) precipitating ion and electron data to study the differences in the equatorward precipitation boundaries of the two populations on the dawnside and duskside of the auroral oval. The large geometric factors for the electron and ion detectors on DMSP make the accurate determination of the boundaries possible. We show that there are systematic differences which are almost always present. The differences are such that the boundaries can be reasonably represented by two circles offset in the dawn-dusk direction with the ions (electrons) reaching lower latitudes on the duskside (dawnside). To explain these patterns, we conclude that for ion boundary formation the time constants for pitch angle diffusion and for convection need to be explicitly taken into account. The constants may be highly dependent on energy, as has already been pointed out by *Ejiri* [1978]. We will point

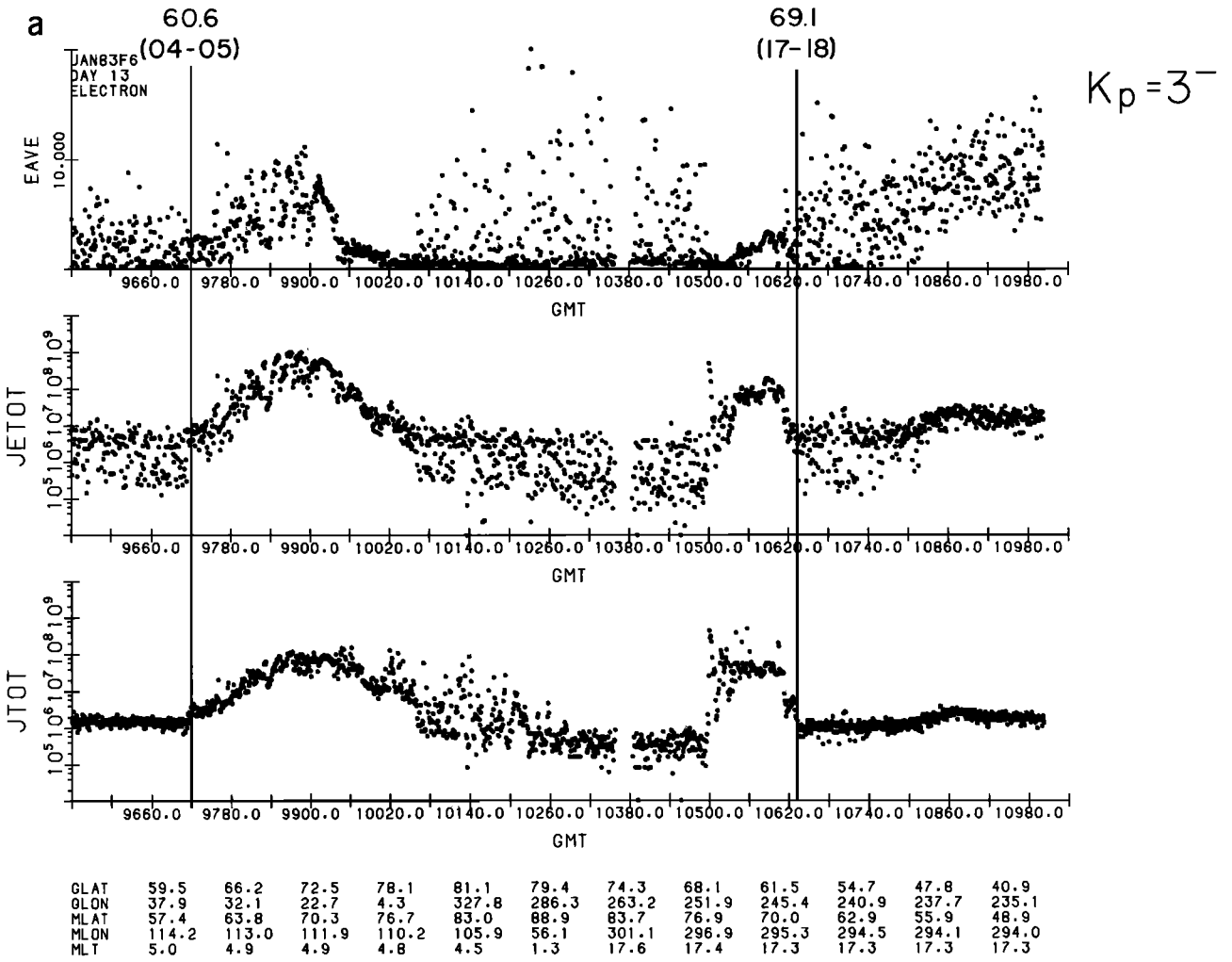

Fig. 2*a*. Integral flux in $(cm^2\ s\ sr)^{-1}$ (bottom panel), energy flux in keV/cm^2 s sr (middle panel), and average energy in keV (top panel) of precipitating electrons measured by the DMSP F6 satellite passing over the north pole on January 13, 1983. These values are plotted as functions of universal time (in seconds), geographic latitude and longitude, corrected geomagnetic latitude and longitude, and magnetic local time. The magnetic coordinates are projected along the magnetic field to an altitude of 110 km. The vertical lines at 60.6° and 69.1° indicate the morning and evening electron equatorward auroral boundaries.

out features of electron and ion precipitation on the boundaries which support these conclusions.

2. Orbit and Instrumentation

DMSP F6 is a three-axis-stabilized satellite, launched into a sun-synchronous, dawn-dusk, circular orbit in December 1982. The altitude of the satellite is 840 km, the orbital period is 101 min, and the nominal inclination is 98.7°. Owing to the offset between the earth spin axis and the magnetic axis, the orbit covers a significant range in magnetic local time (MLT)–corrected geomagnetic latitude (MLAT) coordinates. This coverage is shown in Figure 1. The south pole orbital coverage (dashed line) is offset from the pole toward magnetic local noon; the north pole orbital coverage (solid line) is offset toward magnetic local midnight.

The SSJ/4 sensor on DMSP F6 (also flown on F7, and scheduled for F8 through F14) consists of four cylindrical curved plate electrostatic analyzers arranged in two pairs, one pair to measure electrons and one pair ions. Each pair measures the particle fluxes in 20 energy channels between 30 eV and 30,000 eV. The apertures of the analyzers always face local vertical such that at auroral and polar cap latitudes they detect precipitating, rather than backscattered or trapped particles. The analyzers for ions and electrons are identical except that the polarities on the plates are opposite and the low-energy ion apertures are larger than the low-energy electron apertures. One electron (ion) analyzer covers the energy range from 30 eV to 1 keV with a geometric factor of 2.2×10^{-4} cm^2 sr (3.2×10^{-2} cm^2 sr) and a $\Delta E/E$ of 9.8% (9.8%). The other electron (ion) analyzer covers the energy range from 1 to 30 keV with a geometric factor of 8.7×10^{-4} cm^2 sr (8.6×10^{-4} cm^2 sr) and a $\Delta E/E$ of 9.3% (9.3%). For ions the geometric factors of this instrument are unusually large in comparison to others flown at comparable altitudes, resulting in count levels well above background in the auroral oval. Both electron and ion detectors employ postacceleration (100 V for electrons; 1000 V for ions) to insure unit channeltron efficiency at low energies. A complete 20-point spectrum for

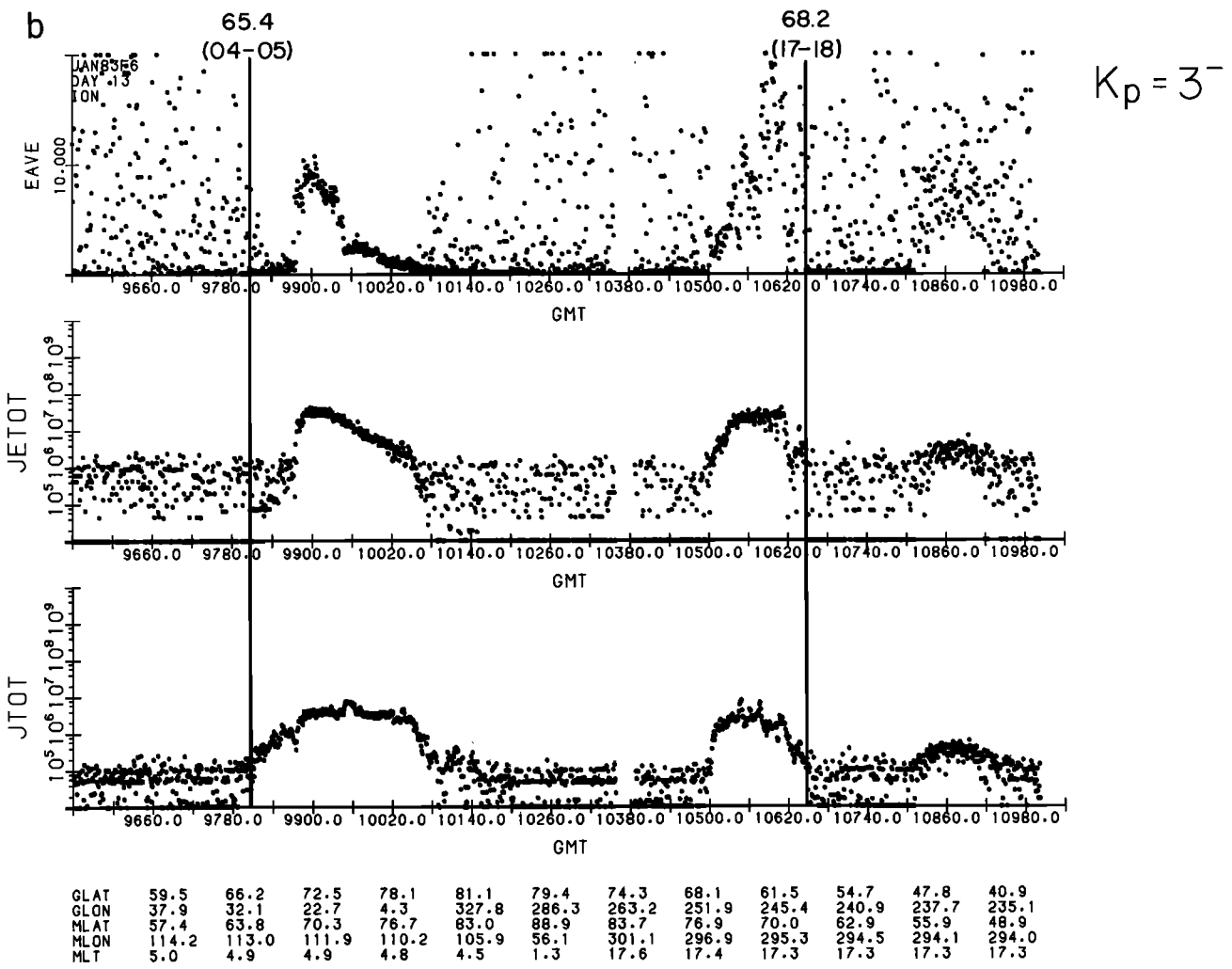

Fig. 2*b*. Same as Figure 2*a* for ions, with the vertical lines at 65.4° and 68.2° indicating the morning and evening ion equatorward auroral boundaries.

both electrons and for ions is returned once per second. Details of the detector and its calibration are given by *Hardy et al.* [1984].

3. Data Selection and Data Base

Figures 2*a* and 2*b* are survey plots of the SSJ/4 electron and ion data, respectively, for a DMSP F6 north polar pass on January 13, 1983, during which *Kp* was 3−. In each figure, three quantities are plotted from top to bottom as a function of universal time in seconds: the particle average energy (EAVE) in keV, the particle total energy flux (JETOT) in keV/cm^2 s sr, and the total particle number flux (JTOT) in particles/cm^2 s sr. At 2-min intervals the bottom of the figure is annotated with the satellite's geographic latitude and longitude; and the corrected geomagnetic latitude (MLAT), longitude, and magnetic local time (MLT), projected along the magnetic field to 110 km. For the pass shown in Figure 2 the satellite traversed the morning auroral oval (0400–0500 MLT), the polar cap (up to 88.9° MLAT), and the evening oval (1700–1800 MLT). The slight rise in the flux level from 10800 to 10980 s UT results from a low level of counts in the detector from penetrating particles from the radiation belts.

In Figure 2 the equatorward precipitating electron and ion boundaries are indicated by vertical lines. The criteria which are used for selection of electron boundaries from these data have been extensively documented [*Gussenhoven et al.*, 1981, 1983] and will not be repeated here. The electron boundaries, in this case, are unambiguous and are at 60.6° MLAT in the 0400–0500 MLT zone and 69.1° MLAT in the 1700–1800 MLT zone.

In Figure 2*b* the ion boundaries are also clear and are chosen from increases in JTOT above equatorward background values. The boundaries chosen are at 65.4° MLAT in the 0400–0500 MLT zone and 68.2° MLAT in the 1700–1800 MLT zone. Typically, the ion flux increases rapidly with increasing latitude at the boundary, and the boundaries are easy to determine. There are cases, however, in which the ion number flux fluctuates widely at the equatorward edge of precipitation, with the fluctuations extending over several degrees of latitude. The latitudinal extent of these fluctuations is larger than in corresponding cases for electrons, and even though the fluctuations are at low flux levels, the boundary was chosen at the lowest latitude to which the fluctuations extended. On occasion, the diffuse auroral ion precipitation on one side of the oval appeared as a double or divided population (i.e., two regions of elevated flux separated by a region at or near background flux levels). This occurred more frequently on the mor-

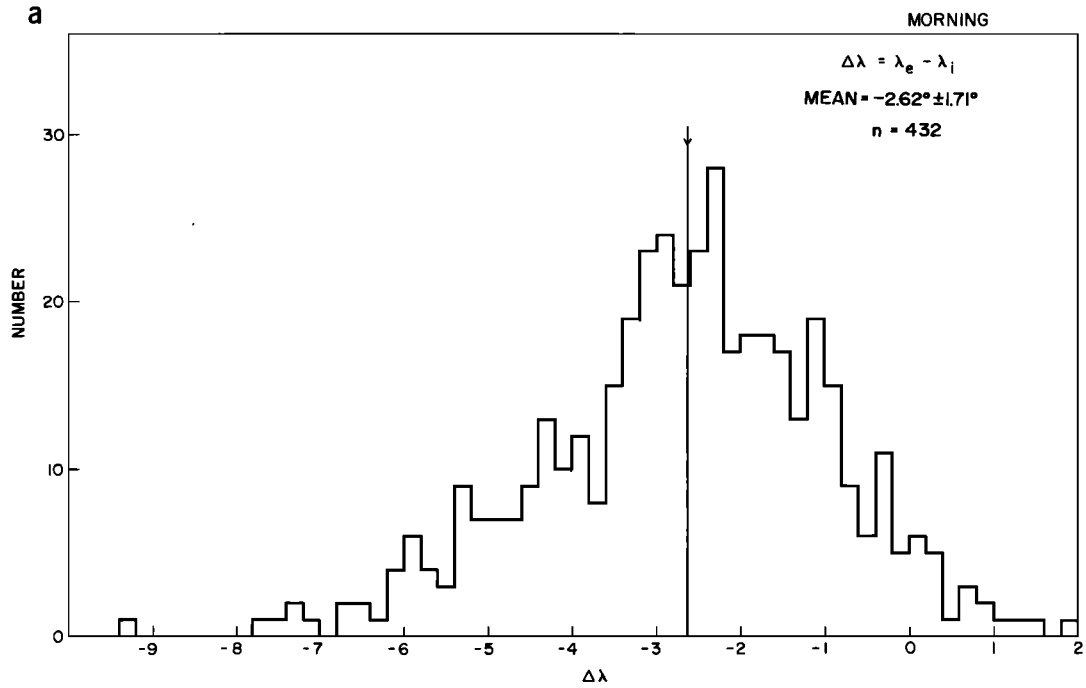

Fig. 3*a*. Occurrence plot for differences, $\Delta\Lambda = \Lambda_e - \Lambda_p$, between all electron and ion boundary pairs measured on the morningside. Values of $\Delta\Lambda$ are binned in units of 0.2° MLAT. The vertical line shows the mean difference.

ningside. In these cases the boundary was chosen for the region at the lower latitudes.

The latitudinal variations in the average energy of the precipitating electron and ion boundaries that are presented in Figure 2 are typical of dawn-dusk DMSP passes. For ions the average energy reaches higher values in the evening auroral oval than in the morning. For electrons the average energy varies in the opposite sense. On both sides of the oval the

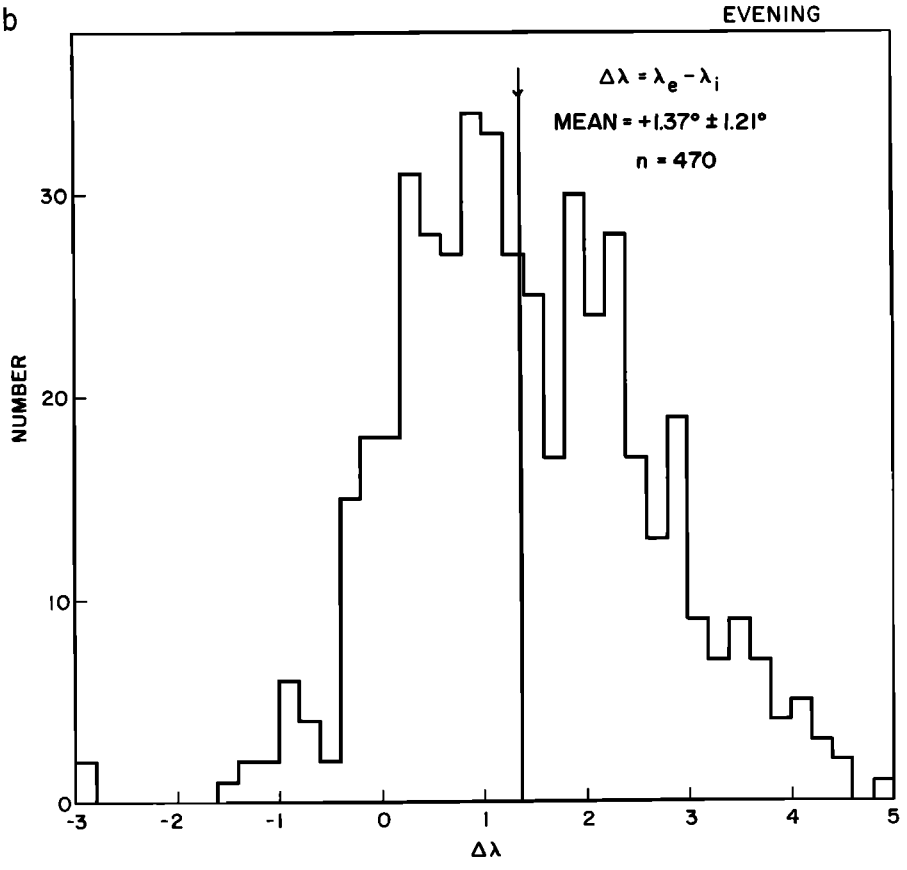

Fig. 3*b*. Same as Figure 3*a* for electron and ion boundary pairs measured on the eveningside.

TABLE 1. Boundary Separation by *Kp*

Kp	Mean (Morning)	Mean (Evening)
0–2+	$-2.72° \pm 1.73°$ ($n = 184$)	$+1.45° \pm 1.13°$ ($n = 288$)
≥3−	$-2.55° \pm 1.70°$ ($n = 248$)	$+1.30° \pm 1.28°$ ($n = 271$)

electron average energy is generally smaller than the ion average energy. This behavior is the same as that found for the source populations measured at near-geosynchronous orbit [*Garrett et al.*, 1981; *Mullen and Gussenhoven*, 1983]. It is consistent with convective motion in a dawn-dusk electric field when the ions and electrons have a common, uniform source in which the initial electron average energy is less than the initial ion average energy. In Figure 2 the electron average energy on both sides of the oval increases with increasing latitude from the equatorward boundary. Generally, the dispersion is much smoother than in the case shown here. This variation is also consistent with convective motion, since the radial distance from the earth of electron Alfvén layers increases with increasing energy. By contrast, on the eveningside of the oval the ion average energy increases abruptly at the equatorward edge and then decreases. (In Figure 2 there is a small spur of low-energy flux ions which has also been included in choosing the evening boundary.) On the equatorward edge of the morning oval there is a relatively broad region of low (less than 1 keV) average energy, low number flux ions extending for several degrees before the sharp onset of a hot ion population. *Sauvaud et al.* [1981] have reported that this cold ion population on the morningside of the oval is observed following increases in *AE* (substorms). These authors pointed out the difficulty in assessing the degree of consistency these observations have with convective motion in a quasi-static electric field because of the complex, energy-dependent nature of the ion Alfvén boundaries.

For the pass in Figure 2, as is the general case, the electron (ion) boundary lies more equatorward of the ion (electron) boundary on the morningside (eveningside) of the oval.

For this study, the electron and ion boundaries were determined for each DMSP F6 pass in January 1983, giving a set of approximately 900 boundaries for ion precipitation and the same for electrons. For each pair of ion and electron boundaries the appropriate *Kp* value was assigned; the difference between the two boundaries, $\Delta\Lambda = \Lambda_e - \Lambda_i$, was determined; and the boundaries and their differences were binned in 1-hour local time zones. Boundaries were excluded from the data set if the electron and ion boundaries in a given pair occurred in different local time bins; 15% of the morning boundaries and 6% of the evening boundaries had such differences. Many of these cases occurred on the dayside where the satellite cuts the auroral oval obliquely. Magnetic local time zones for which there were at least 100 boundaries were 0400–0700 MLT and 1700–2100 MLT. For these zones, data were available for a *Kp* range from 0+ to 5, and linear regressions were performed on the boundary values against *Kp*.

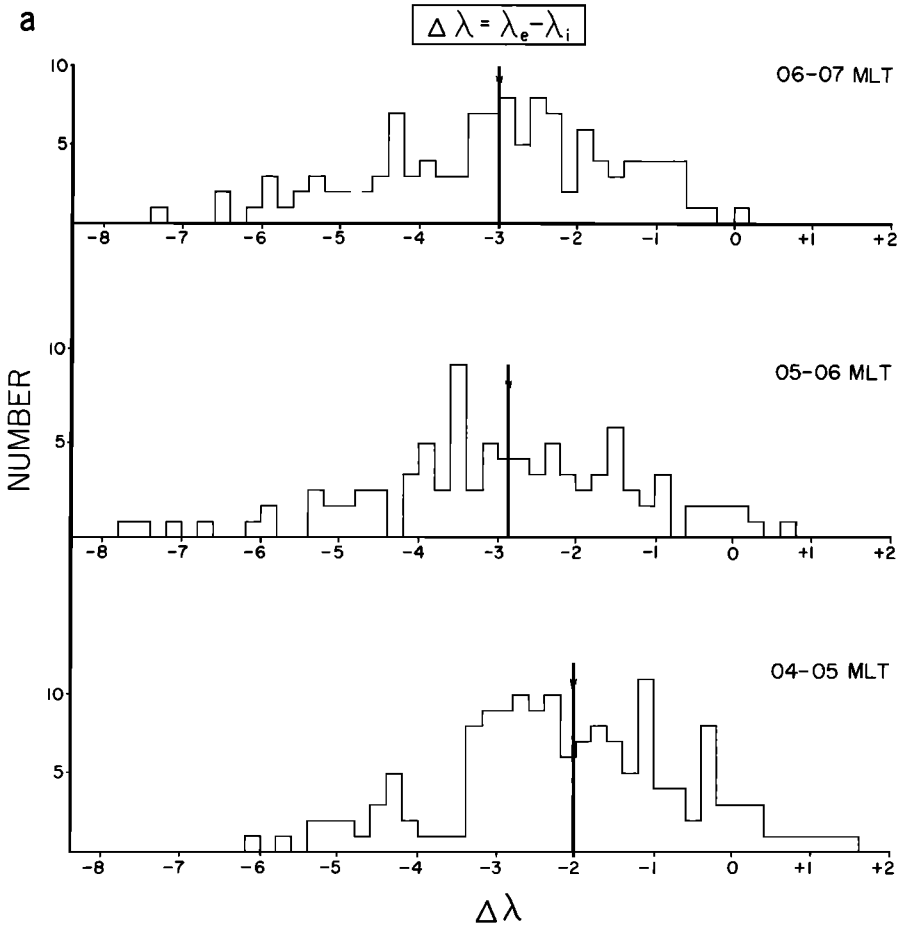

Fig. 4*a*. Same as Figure 3*a* but separated into 1-hour MLT bins.

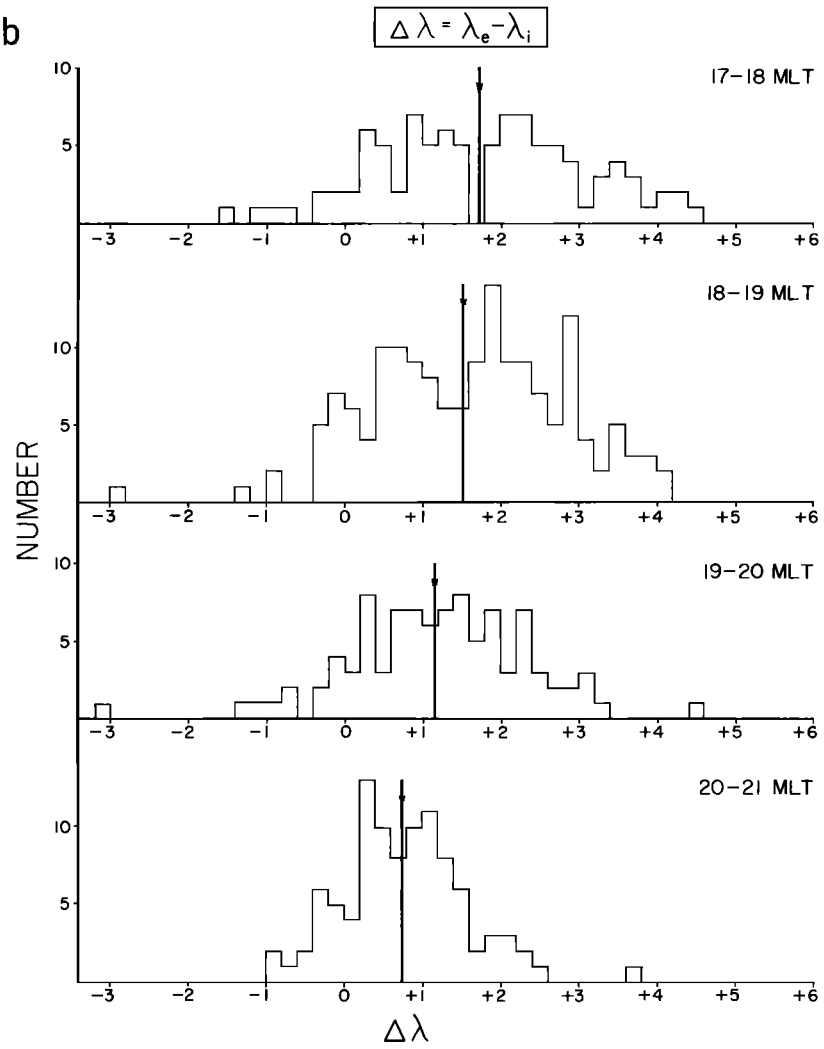

Fig. 4*b*. Same as Figure 3*b* but separated into 1-hour MLT bins.

4. Ion and Electron Boundary Differences

We illustrate the systematic variations in the equatorward boundaries using all of the January 1983 data. Figures 3*a* and 3*b* are occurrence plots of ΔΛ for morning and evening boundary pairs, respectively. Boundaries for the entire MLT and *Kp* ranges are used, and the boundary differences (ΔΛ) are binned in units of 0.2° MLAT. Figure 3*a* shows that with few exceptions the morning electron boundary occurs at lower latitudes then the ion boundary. Of the 432 boundaries, 15 electron boundaries are higher than ion boundaries (3%), and 11 coincide (2.5%). The average difference is $-2.62° \pm 1.71°$ MLAT, which is indicated by the vertical line in Figure 3*a*. For the evening boundaries (Figure 3*b*) the reverse is observed: the ion boundaries occur at lower latitude than the electron boundaries, with 34 of the 470 boundaries (7%) higher and 36 (8%) coincident. The average difference is $+1.37° \pm 1.21°$ MLAT.

We next consider the variation in the difference with *Kp* and MLT. The data were separated into two *Kp* ranges, 0 to 2+, and ≥3−, and the averages of the differences in electron and ion boundaries for the morningside and eveningside of the oval were again calculated. The results are given in Table 1. The differences between the averages of the two *Kp* ranges are small: 0.18° on the morningside, and 0.13° on the eveningside, indicating no activity dependence.

Figures 4*a* and 4*b* are occurrence plots for ΔΛ as a function of local time in 1-hour zones for morning and evening boundary pairs, respectively. In both figures the local time zone closest to midnight is plotted in the bottom panel, moving toward dayside in the upper panels. As in Figure 3, the average ΔΛ is indicated by a vertical line in each panel. Figure 4 shows that the closer the MLT zone is to midnight, the smaller the average divergence between the electron and ion equatorward boundaries. Not only does the average difference between the boundary pairs increase for MLT zones on the dayside, but the spread in the distribution of differences also tends to increase.

Finally, we performed a linear regression on all boundary points in a given MLT zone with *Kp*. In Figures 5*a* and 5*b* the linear fit to the data is shown for the 0400–0500 and the 1800–1900 MLT zones, respectively. The average boundary values for each *Kp* value are plotted as solid (open) circles for electron (ion) boundary averages. (Note: the linear regressions were performed on the full data set in each zone, not on the averages.) Like the electron boundaries, the equatorward edge of the ion precipitation expands to low latitude with increasing *Kp*. In addition, the offset between the electron and ion

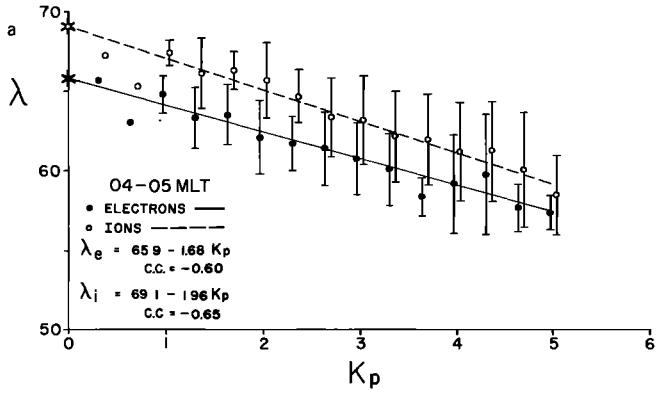

Fig. 5a. Mean values and standard deviations in each Kp bin for electrons (solid circles) and ions (open circles) as a function of Kp for the 0400–0500 MLT sector. The solid (dashed) line results from a linear regression performed with individual boundary determinations of electrons (ions).

boundaries exists over the entire Kp range sampled. The 0400–0500 MLT equatorward electron boundaries are on average about 2°–3° lower than the ion boundaries; and the 1800–1900 MLT equatorward electron boundaries are 1°–2° higher than the ion boundaries. The linear regression results for the MLT zones in which there are ~100 boundaries are given in Table 2. Here, n is the number of boundaries in the given MLT zone, Λ_0 is the intercept at $Kp = 0$, α is the slope in degrees of MLAT per unit Kp, and cc is the correlation coefficient.

The electron results can be compared to those previously published for the DMSP F2 and F4 data in which a much larger data set was used [*Gussenhoven et al.*, 1981, 1983]. Because the distribution of boundaries in Kp range is narrower here than in these earlier studies, the correlation coefficients are somewhat smaller than for the larger data set. In addition, in the earlier studies the evening electron boundaries had negative slopes that increased with MLT toward midnight. In this study, no such consistent trend is found. We attribute these differences to the small data samples and the nonuniform distribution of boundaries in Kp. Similarly, the regression values for ions should only be taken as preliminary. Further statistical studies of the characteristics of the auroral ion boundary are currently in progress.

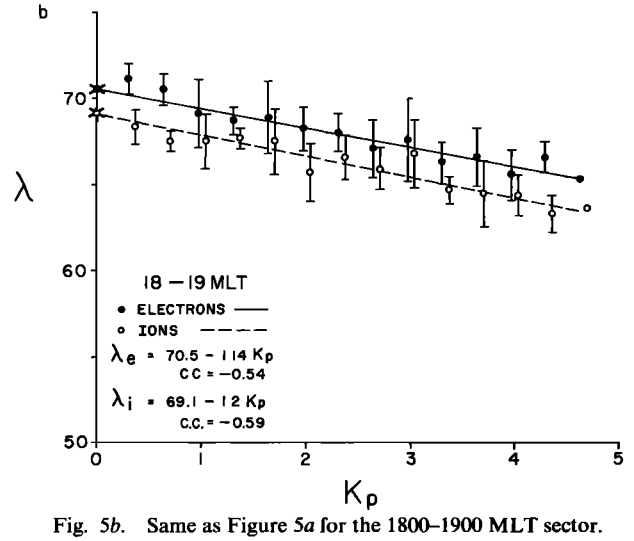

Fig. 5b. Same as Figure 5a for the 1800–1900 MLT sector.

TABLE 2. Linear Regression Results

	Electrons				Ions			
MLT	N	Λ_0	α	cc	N	Λ_0	α	cc
0400–0500	179	65.9	−1.68	−0.60	176	69.1	−1.96	−0.65
0500–0600	130	66.7	−1.62	−0.61	113	69.7	−1.59	−0.62
0600–0700	132	67.5	−1.57	−0.53	118	70.0	−1.30	−0.54
1700–1800	96	72.5	−1.45	−0.64	104	70.7	−1.40	−0.64
1800–1900	160	70.6	−1.16	−0.55	162	69.1	−1.20	−0.59
1900–2000	99	71.4	−2.01	−0.72	108	69.5	−1.75	−0.71
2000–2100	109	68.8	−1.17	−0.55	97	67.9	−1.10	0.55

5. Conclusions and Discussion

From the measurement of approximately 1800 electron and ion boundaries in January 1983 we determined the following:

1. The systematic variation of the equatorward boundary of ion precipitation with magnetic activity is similar to that of the equatorward boundary of electron precipitation: both boundaries move to lower latitudes in a regular fashion with increasing magnetic activity measured by Kp.

2. On the morningside of the oval, from 0400 to 0800 MLT, the electron equatorward boundary is, on average, 2.6° MLAT lower than the equatorward ion boundary.

3. On the eveningside of the oval, from 1700 to 2200 MLT, the equatorward electron boundary is, on average, 1.4° MLAT higher than the equatorward ion boundary.

4. The difference between the electron and ion equatorward boundaries is not a function of Kp.

5. The difference between the equatorward electron and ion boundaries on both morningside and eveningside of the oval increases with local time toward noon.

The electron and ion boundaries, for each level of activity, can be modeled by two circles offset from the geomagnetic pole and each other. That a circular fit to the electron boundary is a good approximation has been shown by *Gussenhoven et al.* [1983]. The electron boundary from *Gussenhoven et al.* [1983] is reproduced in Figure 6 for Kp 0 (5) by the heavy solid (dashed) line along with the average values of the electron boundaries from the present study (crosses) for Kp 0 (5). The morning values lie close to the circles, while the evening values fall at slightly higher latitudes. The average ion boundary values are also shown in Figure 6 (solid circles) and are fit to circles. For the ion circles the centers are along the midnight meridian (the electron centers are on the 0240 MLT meridian) and at the same latitude as the electron circle centers (87.6° and 85.8° for Kp 0 and 5, respectively).

At least three approaches can be taken to interpret the electron and ion boundary differences in the context of large-scale convective motions in a dipole magnetic field.

The first is to self-consistently calculate the electric field and particle motions using only exteriorly imposed boundary conditions. *Karlson* [1971] performed such a calculation with a highly idealized, two-component (defined by temperature) population for both electrons and ions. He assumed a dipole magnetic field and confined the calculation to the equatorial plane. He found that the resulting statistically formed forbidden regions (equatorial boundaries) for the hot populations were offset circles, in the same direction that we measure. The changes in the self-consistently generated cross-tail electric

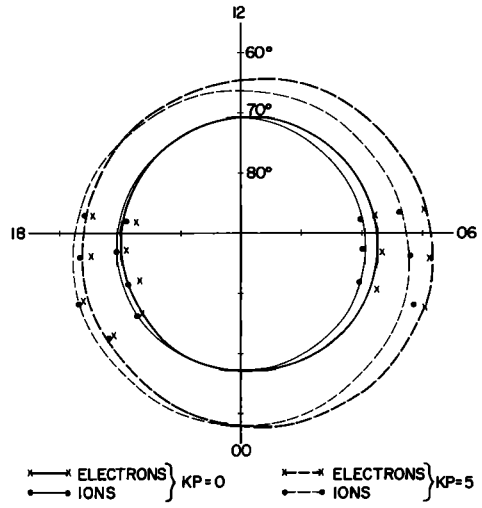

Fig. 6. Circular fits to electron (ion) boundaries for Kp 0 and 5 from *Gussenhoven et al.* [1983] (data set presented here).

field from a constant value are small except at the boundary of the forbidden region. Only general features of the system were expected from such a calculation because of the many simplifying assumptions made. Alternatively, R. A. Wolf et al. (Effects of magnetospheric convection on the magnetic structure of the near magnetotail, submitted to *Journal of Geophysical Research*, 1986) calculated self-consistent near-earth tail magnetic fields from imposed electric fields to show the time-dependent generation of plasma and field conditions for instabilities as an explanation for substorm development. Although there is no question concerning the superiority of nonlinear, self-consistent approaches to plasma sheet dynamics over linear ones, they are very difficult to execute to the degree that they give quantitative results suitable for comparison to measurement.

A second approach to explaining the measured boundary differences is to assume that the ion source region is the ionosphere, while the electron source region remains the plasma sheet. Evidence that the major ion population on the equatorward edge of the morning oval is oxygen rich (ionospheric in origin) has been given by *Sauvaud et al.* [1985]. Trajectory calculations for upwelling ions in a convection electric field are not detailed enough, as yet, for direct comparison to measurement.

A third approach, and one that we examine more closely, assumes that static models for the large-scale cross-tail electric field, such as those proposed by *Volland* [1973], *Stern* [1975], *Ejiri et al.* [1978], and *Baumjohann et al.* [1985], are reasonably correct for the appropriate levels of magnetic activity, and that the near source of the low-altitude populations precipitating at the equatorward edge of the auroral region is the central plasma sheet. In these models any polarization charge that results from differences in the ion and electron motions is removed by a nonauroral particle source. The currents required to balance the polarization charge are in the right sense for region 2 Birkeland currents. In these models the overall forbidden region for ions is always smaller than for electrons. That is, in the completely static case, ions penetrate at all local times to radial distances within the plasmapause. To explain why they are not seen there except on the eveningside, and even there not to the extent predicted, requires more careful examination of time constants of drift and pitch angle diffusion.

We reformat the calculations of *Ejiri* [1978] to illustrate this. They are shown in Figure 7. In his calculations, ions are started at $L = 10$ from 2000 to 0400 MLT in a cross-tail electric field that is 0.57 mV/m at $L = 10$, with a radial dependence such that the plasmapause at the stagnation point is at $L = 5$ (representative of a Kp level of 4). The magnetic field is a dipole. In the two panels of Figure 7 we show the advancing fronts of ions in the ecliptic plane, for four values of the magnetic moment, $\mu = 0$, 13, 52, and 206 eV/nT, and for two different elapsed times, 1 and 4 hours. Ions that are more field aligned will have similar fronts but will lie closer to the earth. Particles of all μ values on the $L = 10$ crescent will fall on separate fronts according to their μ value. The $\mu = 0$ case is also appropriate for electrons and can be thought of as the advancing front for the whole electron population since higher energies will be dispersed behind this front. The teardrop-shaped plasmapause (also the $\mu = 0$ boundary after an infinitely long elapsed time) from the same calculation is shown in each plot.

Even after 1 hour, and long before the plasmapause has been reached by the zero-energy electrons (and ions), a dispersion in the boundaries in μ occurs that is in the same sense as the dispersion that we measure. The ions advance earthward

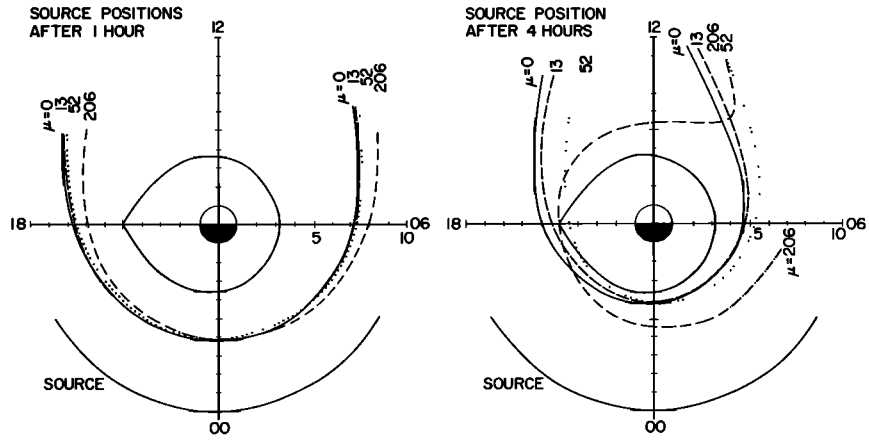

Fig. 7. Boundary fronts in the ecliptic plane for 90° particles of different magnetic moment after 1 and 4 hours of convection electric field drift from a source at 10 R_E.

of the electrons in the evening and fall behind the electrons in the morning. After 4 hours the $\mu = 52$ ions have advanced within the stationary plasmapause (they have an energy of 17.6 keV on the dusk meridian) and are well earthward of the $\mu = 0$ front. On the morningside the $\mu = 52$ ions ($E = 10.8$ keV on the dawn meridian) are well outside both the $\mu = 0$ front and the plasmapause. The lower μ-valued ions have systematic variations in the same sense. The energy-dependent charge fronts in Figure 7 are created solely from energy- and charge-dependent time scales of the convective motion. They are in good agreement with the measurements in the dusk to predmidnight sector, giving the correct energy dispersion, as well. In the postmidnight region, however, they indicate that (1) the electron and ion earthward boundaries should coincide (zero-energy boundaries) and (2) the energy dispersion for the two populations should be in the same sense. Both are in disagreement with the measured precipitation characteristics.

Two additional features of ion transport and loss could bring the observed ion boundaries on the morningside into agreement with convective motions. First, the low-energy plasma sheet ions (in the 1-keV range) could experience less efficient pitch angle diffusion than those with higher energies (the 10-keV range). If this were the case, the low-energy ions would have empty loss cones, and no ions would be observed at low altitudes. This would shift the morning ion boundary poleward and not affect the evening boundary. Second, another source (presumably the ionosphere) could provide a low-energy population earthward of the 10-keV population but beyond the low-energy electron population. This would place warm ions on the equatorward boundary but not restrict them to plasma sheet positions. *Sauvaud et al.* [1985] have presented evidence for this latter process.

Finally, we stress that in our approach to the boundary problem we assume that there is validity in dealing statistically with the cross-tail electric field and particle convection. At the very least this provides an ordering of the importance of various magnetospheric processes. It may be the case that a nonlinear treatment involving charge neutralization, time-dependent E and B fields, wave production, pitch angle diffusion, and loss is inherently more self-ordering. In any case the systematic expansion of both the electron and ion boundaries with increasing magnetic activity, as we have described here, indicates that the system is well ordered.

Acknowledgments. We thank Alice Campbell for the careful work in selecting the boundaries. The work of N. Heinemann was performed under the Air Force Geophysics Laboratory contracts F19628-82-K-0011 and F19628-86-C-0029.

The Editor thanks K. Makita and J. S. Murphee for their assistance in evaluating this paper.

REFERENCES

Alfvén, H., and C.-G. Falthammar, *Cosmical Electrodynamics*, 2nd ed., Oxford at the Clarendon Press, London, 1963.

Ashour-Abdalla, M., and R. M. Thorne, Toward a unified view of diffuse auroral precipitation, *J. Geophys. Res.*, *83*, 4755, 1978.

Baumjohann, W., G. Haerendel, and F. Melzner, Magnetospheric convection observed between 0600 and 2100 LT: Variations with *Kp*, *J. Geophys. Res.*, *90*, 393, 1985.

Cowley, S. W. H., and M. Ashour-Abdalla, Adiabatic plasma convection in a dipole field: Electron forbidden-zone effects for a simple electric field model, *Planet. Space Sci.*, *24*, 805, 1976*a*.

Cowley, S. W. H., and M. Ashour-Abdalla, Adiabatic plasma convection in a dipole field: Proton forbidden-zone effects for a simple electric field model, *Planet. Space Sci.*, *24*, 821, 1976*b*.

Eather, R. H., Auroral precipitation and hydrogen emissions, *Rev. Geophys.*, *5*, 207, 1967.

Ejiri, M., Trajectory traces of charged particles in the magnetosphere, *J. Geophys. Res.*, *83*, 4798, 1978.

Ejiri, M., R. A. Hoffman, and P. H. Smith, The convection electric field model for the magnetosphere based on Explorer 45 observations, *J. Geophys. Res.*, *83*, 4811, 1978.

Feldstein, Y. I., and Yu. I. Galperin, The auroral luminosity structure in the high-latitude upper atmosphere: Its dynamics and relationship to the large-scale structure of the earth's magnetosphere, *Rev. Geophys.*, *23*, 217, 1985.

Fontaine, D., and M. Blanc, Theoretical approach to the morphology and dynamics of diffuse auroral zones, *J. Geophys. Res.*, *88*, 7171, 1983.

Fukunishi, H., Dynamic relationship between proton and electron auroral substorms, *J. Geophys. Res.*, *80*, 553, 1975.

Galperin, Yu. I., V. A. Gladyshev, N. V. Jorjio, R. A. Kovrazhkin, V. M. Sinitsin, F. Cambou, J. A. Sauvaud, and J. Crasnier, Adiabatic acceleration induced by convection in the plasma sheet, *J. Geophys. Res.*, *83*, 2567, 1978.

Garrett, H. B., D. C. Schwank, and S. E. DeForest, A statistical analysis of the low-energy geosynchronous plasma environment, II, Ions, *Planet. Space Sci.*, *29*, 1045, 1981.

Gussenhoven, M. S., D. A. Hardy, and W. J. Burke, DMSP/F2 observations of equatorward auroral boundaries and their relationship to magnetospheric electric fields, *J. Geophys. Res.*, *86*, 768, 1981.

Gussenhoven, M. S., D. A. Hardy, and N. Heinemann, Systematics of the equatorward diffuse auroral boundary, *J. Geophys. Res.*, *88*, 5692, 1983.

Hardy, D. A., W. J. Burke, M. S. Gussenhoven, N. Heinemann, and E. Holeman, DMSP/F2 electron observations of equatorward auroral boundaries and their relationship to the solar wind velocity and the north-south component of the interplanetary magnetic field, *J. Geophys. Res.*, *86*, 9961, 1981.

Hardy, D. A., L. K. Schmitt, M. S. Gussenhoven, F. J. Marshall, H. C. Yeh, T. L. Schumaker, A. Huber, and J. Pantazis, Precipitating electron and ion detectors (SSJ/4) for the block 5D/flights 6-10 DMSP satellites: Calibration and data presentation, *Rep. AFGL TR 84 0317*, Air Force Geophys. Lab., Hanscom Air Force Base, Mass., 1984.

Hultqvist, B., The hot ion component of the magnetospheric plasma and some relations to the electron component—Observations and physical implications, *Space Sci. Rev.*, *23*, 581, 1979.

Kamide, Y., and J. D. Winningham, A statistical study of the "instantaneous" nightside auroral oval: The equatorial boundary of electron precipitation as observed by the ISIS 1 and 2 satellites, *J. Geophys. Res.*, *82*, 5573, 1977.

Karlson, E. T., Plasma flow in the magnetosphere, *Cosmic Electrodyn.*, *1*, 474, 1971.

Lambert, S., and P. R. Sutcliffe, Photometric observations of the proton aurora at Sanae, *J. Atmos. Terr. Phys.*, *43*, 355, 1981.

Lui, A. T. Y., D. Venkatesan, C. D. Anger, S.-I. Akasofu, W. J. Heikkila, J. D. Winningham, and J. R. Burrows, Simultaneous observations of particle precipitations and auroral emissions by the ISIS 2 satellite in the 19–24 MLT sector, *J. Geophys. Res.*, *82*, 2210, 1977.

Makita, K., C.-I. Meng, and S.-I. Akasofu, The shift of the auroral electron precipitation boundaries in the dawn-dusk sector in association with geomagnetic activity and interplanetary magnetic field, *J. Geophys. Res.*, *88*, 7967, 1983.

Mullen, E. G., and M. S. Gussenhoven, SCATHA environmental atlas, *Rep. AFGL-TR-83-0002*, Air Force Geophys. Lab., Hanscom Air Force Base, Mass., 1983.

Nakai, H., Y. Kamide, D. A. Hardy, and M. S. Gussenhoven, Time scales of expansion and contraction of the auroral oval, *J. Geophys. Res.*, *91*, 4437, 1986.

Sauvaud, J. A., J. Crasnier, K. Mouala, R. A. Kovrazhkin, and N. V. Jorjio, Morning sector ion precipitation following substorm injections, *J. Geophys. Res.*, *86*, 3430, 1981.

Sauvaud, J. A., J. Crasnier, Yu. I. Galperin, and Y. I. Feldstein, A statistical study of the equatorward boundary of the diffuse aurora in the premidnight sector, *Geophys. Res. Lett.*, *10*, 749, 1983.

Sauvaud, J. A., J. M. Bosqued, R. A. Kovrazhkin, D. Delcourt, J. J. Berthelier, F. Lefeuvre, J. L. Rauch, Yu. I. Galperin, M. M. Mogilevsky, and E. E. Titova, Positive ion distributions in the morning auroral zone: Local acceleration and drift effects, *Adv. Space Res.*, *5*, 73, 1985.

Schield, M. A., J. W. Freeman, and A. J. Dessler, A source for field-aligned currents at auroral latitudes, *J. Geophys. Res.*, *74*, 247, 1969.

Smith, P. H., and R. A. Hoffman, Direct observations in the dusk hours of the characteristics of the storm time ring current particles during the beginning of magnetic storms, *J. Geophys. Res.*, *79*, 966, 1974.

Southwood, D. J., and S. M. Kaye, Drift boundary approximations in simple magnetospheric convection models, *J. Geophys. Res.*, *84*, 5773, 1979.

Stern, D. P., The motion of a proton in the equatorial magnetosphere, *J. Geophys. Res.*, *80*, 595, 1975.

Stern, D. P., The origins of Birkeland currents, *Rev. Geophys.*, *21*, 125, 1983.

Vallance-Jones, A., *Aurora*, D. Reidel, Hingham, Mass., 1974.

Vallance-Jones, A., F. Creutzberg, R. L. Gattinger, and F. R. Harris, Auroral studies with a chain of meridian-scanning photometers, 1, Observations of proton and electron aurora in magnetospheric substorms, *J. Geophys. Res.*, *87*, 4489, 1982.

Volland, H., A semiempirical model of large-scale magnetospheric electric fields, *J. Geophys. Res.*, *78*, 171, 1973.

M. S. Gussenhoven and D. A. Hardy, AFGL/PHP, Hanscom Air Force Base, MA 01731.

N. Heinemann, Physics Department, Boston College, Chestnut Hill, MA 02167.

(Received September 4, 1986;
revised December 5, 1986;
accepted December 29, 1986.)